Reactions and luminescence in passivated Si nanocrystallites induced by vacuum ultraviolet and soft-x-ray photons

Y. Chao, S. Krishnamurthy, and M. Montalti
School of Chemical Engineering and Advanced Materials, University of Newcastle upon Tyne, Newcastle upon Tyne, NE1 7RU, United Kingdom

L. H. Lie, A. Houlton, and B. R. Horrocks
School of Natural Sciences, University of Newcastle upon Tyne, Newcastle upon Tyne, NE1 7RU, United Kingdom

L. Kjeldgaard
MAX-lab, Lund University, S-22 100 Lund, Sweden

V. R. Dhanak
Council for the Central Laboratory of the Research Councils (CCLRC), Daresbury Laboratory, Warrington, Cheshire, WA4 4AD, United Kingdom and Surface Science Centre, Liverpool University, Liverpool, L69 3BX, United Kingdom

M. R. C. Hunt
Department of Physics, University of Durham, Durham, DH1 3LE, United Kingdom

L. Šiller[a)]
School of Chemical Engineering and Advanced Materials, University of Newcastle upon Tyne, Newcastle upon Tyne, NE1 7RU, United Kingdom

(Received 10 December 2004; accepted 7 July 2005; published online 24 August 2005)

Alkyl-modified silicon nanocrystallites are efficient fluorophores which are of interest for fundamental spectroscopic studies and as luminescent probes in biology because of their stability in aqueous media. In this work we have investigated these particles using scanning tunneling microscopy, synchrotron-radiation excited photoemission, and x-ray excited optical luminescence (XEOL). During the course of illumination with 145-eV photons we have monitored the evolution of the Si2*p* core level and, in samples which have suffered prolonged atmospheric exposure, observed in real time the growth of an extra Si2*p* component attributed to *in situ* photoinduced oxidation of the Si nanocrystallites. XEOL reveals that two emission bands are active upon soft-x-ray photon excitation and that photoluminescence intensity decreases with photon exposure, which is attributed to charge trapping within the film. © *2005 American Institute of Physics*. [DOI: 10.1063/1.2012511]

INTRODUCTION

Semiconductor nanocrystallites, or quantum dots, are potential building blocks of future nanoelectronic and nanophotonic devices. When Si nanostructures become smaller than 20–30 nm, the transport, electronic, and optical properties of bulk silicon start to be influenced significantly by quantum confinement effects.[1] Therefore, it is desirable to develop techniques for fabrication of silicon nanocrystallites (Si-NCs) and to understand their physical and chemical properties. The intensive investigation of Si nanostructures is linked to potential applications in light-emitting devices integrated on a chip.[2,3] Recently, optical gain in silicon nanocrystals embedded in a silicon dioxide matrix has been shown; this brings fabrication of a silicon laser a significant step closer.[4] Compared with the weak IR luminescence of bulk silicon (observed only at low temperatures), the efficiency of photoluminescence (PL) from Si nanostructures is strongly increased due to the greater overlap of electron-hole pairs.[5] Numerous models have been proposed to explain photoluminescence from silicon nanocrystals, such as recombination of quantum confined electron-hole pairs at surface states related to silicon-oxygen or silicon-hydrogen bonds.[6,7]

In this work we have performed a detailed study, using scanning tunneling microscopy (STM), soft-x-ray photoemission and, x-ray excited optical luminescence (XEOL) of alkylated Si-NCs whose preparation and characterization by mass spectrometry and optical luminescence have been previously reported.[8,9] Our studies confirm the diameter of the nanocrystallites and demonstrate that oxidation may be induced at the nanocrystallite surface by irradiation with vacuum ultraviolet/soft-x-ray (VUV/XUV) photons in samples which have suffered prolonged exposure to ambient atmosphere. In addition, our data indicate that charge trapping within the nanocrystallite films, rather than oxidation, plays a key role in the decay of photoluminescence from the material. So far, there are no investigations in the literature of any kind which explore the interaction of photons in the VUV/XUV energy region with Si-NCs. Chemical changes induced by illumination of the nanocrystallites may well be involved in aging processes, for this reason the VUV/XUV

[a)]Author to whom correspondence should be addressed; electronic mail: lidija.siller@ncl.ac.uk

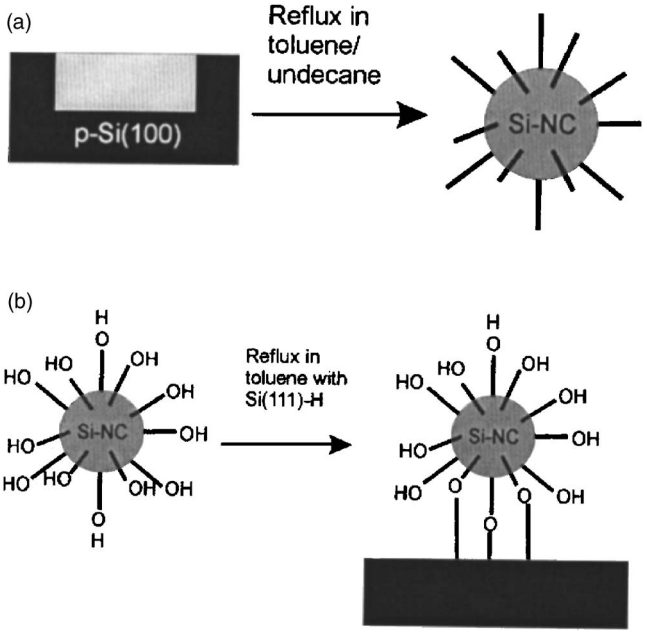

FIG. 1. A schematic diagram showing (a) the break-up of porous silicon during thermal hydrosilylation to form Si–NCs capped with an alkyl (C_{11} =undecyl) monolayer. (b) The reaction of Si–NCs passivated with a hydroxyl-terminated monolayer with hydrogen-terminated Si(111) to anchor the Si–NCs for scanned probe microscopy.

photon energy range is particularly interesting because the Si2*p* core levels are accessible, allowing both the chemical state and luminescence to be followed simultaneously, and their relationship to be determined. The effects of aging in porous silicon have been studied over the past decade (Refs. 10–13, and references therein) and are still a subject of interest in many investigations which aim to discover appropriate capping layers (Refs. 14–16, and references therein) to suppress ambient aging and prepare porous silicon for industrial applications. However, studies of the aging of Si nanocrystallites are rare, and we have found only a few indirect studies.[6,17] The lack of aging studies may be due to previous difficulties in preparation of these materials in sufficient (milligram) quantities for study by conventional spectroscopic techniques.

EXPERIMENT

Details of the electrochemical method used to alkylate the Si nanocrystallites have been published elsewhere,[8] and the resulting material is schematically depicted in Fig. 1(a). The dry powder of silicon nanocrystallites was resuspended by stirring in dichloromethane (CH_2Cl_2) (spectroscopic grade, Sigma-Aldrich) just before preparing the samples investigated in this work, and a few drops of the suspension were cast onto a substrate [either the (0001) face of highly oriented pyrolytic graphite (HOPG), or a gold foil]. The film was then introduced into an ultrahigh-vacuum (UHV) chamber in which typical pressures were below 5×10^{-10} mbar. The resulting samples were then studied by photoemission spectroscopy and XEOL, as detailed below.

Previous estimates for the diameter of the silicon nanocrystallites are 2.8–3.4 nm,[8] which is supported by preliminary high-resolution transmission electron microscopy (HR-TEM) studies.[18] To obtain a more accurate measure of the diameter we have made STM measurements of nanocrystallites dispersed on hydrogen passivated Si(111) surfaces. We use a slightly modified termination for the nanocrystallites examined by STM [compare Figs. 1(a) and 1(b)] due to the mobility of the alkyl-terminated nanocrystallites under imaging—the weak van der Waals interactions between the nanocrystallites and the hydrogen passivated substrate are insufficient to prevent motion induced by the STM tip during scanning. Nanocrystallites passivated by a hydroxyl-terminated monolayer can be anchored to the surface as described below, enabling microscopy investigations, but are otherwise identical to the alkyl-terminated nanocrystallites [Fig. 1(a)] used in the spectroscopic studies.

The hydrogen passivated Si(111) surface was prepared by a deoxygenated NH_4F etch in which ⟨111⟩-oriented silicon wafers (phosphorus-doped, *n*-type, 1–20-Ω cm resistivity, $<0.1°$ miscut, Compart Technology, Peterborough, UK) were first cut into 1-cm^2 square pieces and then degreased with trichloroethylene followed by acetone. An oxide layer was formed by immersing the samples in freshly prepared "piranha" solution (4:1 *v*/*v* concentration H_2SO_4 and 30% H_2O_2) for 1 h at 80 °C. The oxide was removed and a hydrogen-terminated surface was formed by etching in N_2-sparged 40% *w*/*v* aqueous NH_4F for 20 min with the sample held in a vertical orientation. Wafers were then rinsed in de-ionized water (Millipore, nominal 18-MΩ cm resistivity) and blown dry with N_2. Hydroxyl-terminated nanocrystallites were prepared using dimethoxytrityl-protected undecenol in place of undecene in the hydrosilylation procedure for formation of the nanocrystallites. First, dimethoxytrityl-protected undecenol was reacted with the porous silicon layer under conditions of refluxing toluene as described previously[9,19] to produce a layer of porous silicon modified by a monolayer of the protected alcohol. The hydroxyl groups were then exposed by cleaving the trityl protecting group in HF/EtOH prior to cleaving the nanocrystallites from the porous silicon surface. This results in the formation of Si-NCs passivated by a hydroxyl-terminated alkyl monolayer [see Fig. 1(b)]. The hydrogen passivated Si(111) surface reacts with the hydroxyl groups of the Si-NCs under conditions of refluxing toluene to form Si–O–C linkages[20] suitable for anchoring the nanocrystallites for probe microscopy investigations.

Figure 2(a) show a 1×1-μm^2 STM image of silicon nanocrystallites covalently attached to a Si(111) surface. The tunneling current was 66 pA with a bias voltage of 1.5 V, and the samples were imaged under ambient conditions. The STM images show the usual monoatomic steps and wide terraces. Evidence for two-dimensional islanding of the nanocrystallites is reflected in the differing lateral extent of the raised topographic features. The height of the islands is ca. 4–5 nm [See Fig. 2(b)] which is in agreement with previous estimates of the diameter of the Si core from Raman spectroscopy [2.5 nm (Ref. 9)] plus the thickness of the C_{11} alkyl chains.

Soft-x-ray photoemission spectra were acquired at beamline I511 of MAX-Lab, Lund, Sweden and both photoemission and XEOL spectra were measured at beamline 4.1 of the

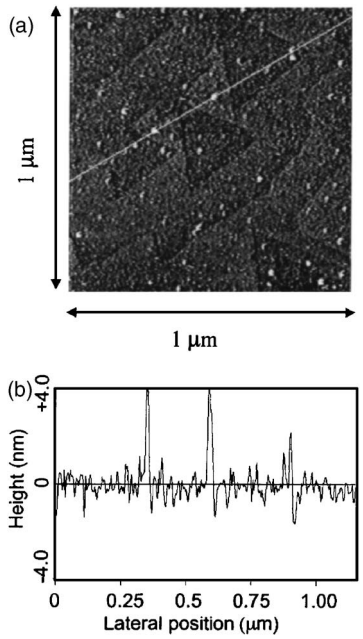

FIG. 2. (a) 1×1-μm^2 STM image of silicon nanocrystals dispersed on hydrogen-passivated Si(111). The sample was prepared by refluxing Si–NCs passivated with a hydroxyl-terminated monolayer with hydrogen-terminated Si(111). The tunneling current was 66 pA and the bias voltage was 1.5 V. The sample was imaged in air. (b) Line profile across the diagonal of the STM image in (a).

synchrotron-radiation source (SRS), Daresbury, UK. In all photoemission spectra, binding energies are referred to the $4f$ photoemission lines measured on a gold foil in direct electrical contact with the sample, with the binding energy of the Au $4f_{7/2}$ line defined as 84.0 eV.[21] It should be noted that all the films measured display some degree of charging, ultimately reaching a stationary state, as discussed below. Consequently, the "binding energies" quoted do not reflect the true binding energies of the core-level photoelectrons, but incorporate the energy required for the electrons to escape the surface charge distribution. However, the degree of charging is small and does not prevent identification of the elemental composition and chemical state of the silicon nanocrystallites, which are considered later. Photoluminescence spectra were obtained using a SPEX 1681B 0.22-m spectrometer with a Hamamatsu Model H957 photomultiplier module (built-in PMT R928). A Keithley 617 programmable electrometer was used to detect the photomultiplier current and the whole system controlled by a personal computer. The particular photomultiplier tube used was chosen for its flat response in the wavelength range investigated. All luminescence and photoemission data were recorded at room temperature. Two "types" of sample were studied, differing in their history: the first was rapidly inserted into the UHV chamber whereas we kept the second type of samples in air for several hours before introduction into the vacuum, we refer to these as "fast" and "slow" samples, respectively. Measurements were repeated on a number of samples of both types and found to be reproducible.

RESULTS AND DISCUSSION

Figure 3(a) shows the development of normalized Si2p spectra obtained in normal emission, with 145-eV photons,

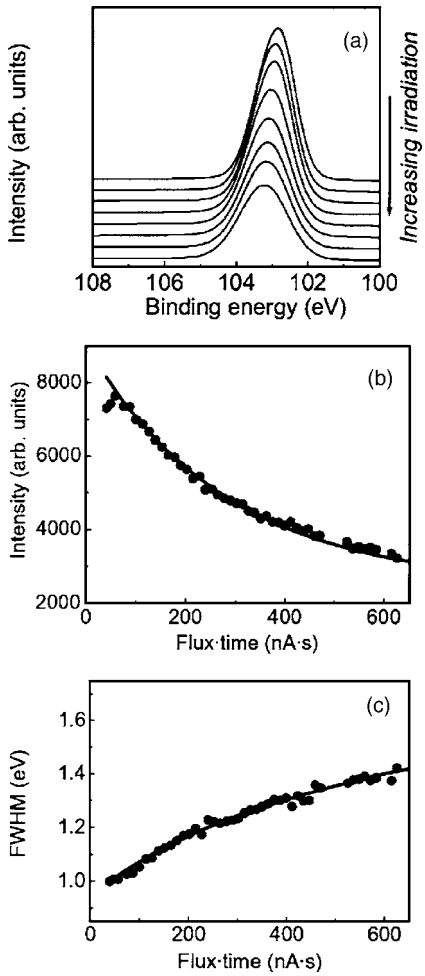

FIG. 3. (a) Si2p spectra obtained at normal emission with 145-eV photons from a Si-nanocrystallite film rapidly introduced into the vacuum chamber. ("fast" sample). (b) The intensity of the Si2p peak as a function of irradiation. The line is an exponential decay fitted to the data. (c) A plot of the evolution of the FWHM of the Si2p peak as a function of irradiation.

for a sample which was introduced rapidly (a fast sample). The spectra are normalized to photon flux. A single peak is observed over the whole dose range studied. Initially located at a binding energy of 102.8 ± 0.1 eV, the peak moves upwards in binding energy to 103.2 ± 0.1 eV after irradiation. The variation of the intensity of the Si2p peak with photon exposure is plotted in Fig. 3(b). We see that the intensity falls exponentially, and can be modeled by the relationship $I_{\mathrm{PES}}=6500\exp(-x/280)+2500$, where $x=\mathrm{flux}\times\mathrm{time(nA\ s)}$. In Fig. 3(c) the variation in the peak width (full width at half maximum) is plotted as a function of time. The full width at half maximum (FWHM) of the peak increase with irradiation and follows a logarithmic function, $\mathrm{FWHM}=\ln[(x+200)/12]/3$, where $x=\mathrm{flux}\times\mathrm{time(nA\ s)}$. Exponential decay of intensity and broadening of photoemission peaks is a normal fingerprint of charging phenomena.

Figure 4(a) shows the development of Si2p spectra obtained in normal emission, with 145-eV photons, for a sample that had been exposed to the air for several hours (slow sample). The spectra are normalized to photon flux. Initially a single peak (denoted A) is observed at a nominal binding energy of 103.5 ± 0.1 eV. However, upon irradiation

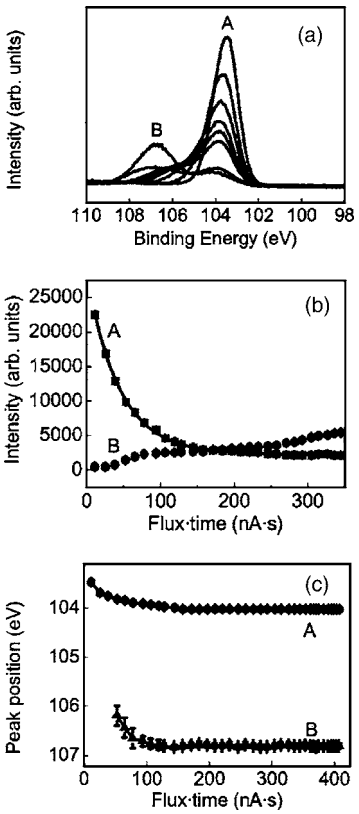

FIG. 4. (a) Si2*p* spectra, obtained at normal emission with 145-eV photons from a Si-nanocrystallite film exposed to air for several hours ("slow" sample). The evolution of the spectra with photon exposure, including the growth of an extra, higher binding-energy peak, is clear. (b) Plot of the intensity evolution of low (peak A) and high (peak B) binding-energy Si2*p* peaks as a function of photon irradiation. The decay in intensity of peak A is fitted with an exponential decay (line) (see text for details). (c) The evolution of the binding energies of the two Si2*p* lines as a function of photon exposure.

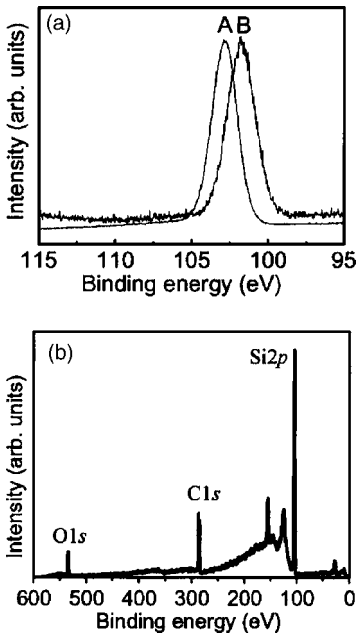

FIG. 5. (a) Si2*p* spectra obtained in normal-emission geometry with 145-eV photons at room temperature showing a "fast" sample as introduced (peak A) and after annealing to 275 °C for 5 minutes (peak B). (b) A survey spectrum measured in normal emission with 633-eV photons for a "fast" sample after heating to ~275 °C for 5 min.

this peak decreases in intensity and shifts to higher binding energy. The change in position and intensity of the peak at 103.5 eV is accompanied by the growth of a "tail" at higher binding energy which also grows in relative intensity and moves progressively to higher binding energy. Eventually the tail develops into a clear peak at a final binding energy of approximately 106.8±0.1 eV. Figure 4(b) shows the development of the intensity of both peaks with irradiation, measured in terms of flux×time. The decay of the intensity of the peak initially located at 103.5±0.1-eV binding energy (I_{PES}) may be fitted to an exponential function: $I_{\mathrm{PES}} = 26\,600\exp(-x/44)+2200$, where $x=\mathrm{flux}\times\mathrm{time(nA\ s)}$. The incident photon flux was measured with a gold grid held immediately before the main experimental chamber, and although the scale is internally consistent, we cannot convert the exposure simply into the number of photons per square meter because we do not exactly know the solid angle and distance between the mesh and the sample, and thus the lifetime determined from the fitting is only a qualitative measure. As this initial peak decays the second peak is seen to continuously rise during the course of irradiation. The development of the binding energy of the two peaks during exposure to synchrotron radiation is shown in Fig. 4(c). Peak A moves from its initial position of 103.5±0.1 eV before saturating at a binding energy of 104.0±0.1 eV, while the position of the second peak (labeled B) shifts, from 106.2±0.2 eV, to a saturation binding energy of 106.8±0.1 eV. The initial position of peak A differs between the fast and slow samples having binding energies of 102.8±0.1 eV vs 103.5±0.1 eV, respectively. However, slightly different binding-energy values are expected since the thickness of the Si–NC film may vary in each deposition from the solution of quantum dots, which would influence the degree of charging within the film. It is notable that even after several hours of photoirradiation no extra peak is observed for the fast sample, contrary to the behavior of the slow sample.

In Fig. 5(a) we plot the Si2*p* region of a fast sample (in the spectra shown the nanocrystallite film was deposited on a HOPG substrate) at room temperature [spectrum A] and after heating to ~275 °C for 5 min [spectrum B]. Valence-band spectra (not shown here) demonstrate emission from the substrate after annealing (absent before the anneal), leading to the conclusion that upon annealing at temperatures of ~275 °C the Si–NCs begin to desorb from graphite. In particular, the desorption[22] leads to a thinning of the Si–NC film and a reduction in charging due to the proximity of the graphite surface to the remaining Si–NC material (i.e., screening and neutralization by the substrate is more effective in the thinner film). This is reflected in a shift of the Si2*p* peak to lower binding energy, from 102.9±0.1 eV in the as-introduced film to 101.8±0.1 eV after annealing. The energy position of 101.8 eV is still far from the known position for Si–Si bonds, 99.5 eV,[14] which indicates that even in a thin film there is still considerable charge trapping in the film as soon as irradiation starts, as we will discuss below. The continued presence of charge trapping arises from the passiva-

tion of the Si–NCs by the long alkyl chains and may be further contributed to by the likelihood that the nanocrystallites are still in the form of agglomerated clusters rather than dispersed as individual particles. In Fig. 5(b) a survey spectrum before heating, obtained at a photon energy of 633 eV, is plotted. Si2*p*, O1*s*, and C1*s* core lines are clearly visible, supporting previous infrared (IR) spectroscopy studies, which indicate the presence of both Si–C (anchoring the alkyl chains to the dot) and Si–O bonds [from the oxidation of unalkylated Si–H (Ref. 8)]. Taken together, the data indicate that the silicon nanocrystallites are encapsulated with a combination of surface (sub)oxides and alkyl chains.

We interpret the initial change in Si2*p* binding energies, their final saturation, and the dependence of the binding energy on film thickness as signatures of charging within the film. In consequence, as mentioned earlier, the binding energies quoted do not reflect the real binding energy of the core level in question, referenced to the substrate Fermi level,[23] but include the energy barrier due to local charge-induced fields that the photoelectron must overcome in order to escape from the surface of the nanocrystallite film. The saturation of the charge-induced shifts in binding energies arises from an equilibrium charging within the film which has also been observed in molecular systems such as C_{60}, for example.[24,25] The relatively small change in the width of peak A [Fig. 4(c)] indicates that this surface charging is relatively homogeneous. The presence of dynamic equilibrium charging is likely to arise from the slow neutralization of photoinduced surface charge through charge percolation pathways[26] (such transport is well known in granular systems).[27]

In the slow sample the second Si2*p* component can be observed to evolve with photon irradiation [Fig. 4(a)], and, at the highest photon doses, is separated by 2.8 ± 0.1 eV from the initial line (peak A). Survey spectra indicate that only Si, C, and O are present in the films (there may also be some hydrogen, which cannot be directly detected by photoemission spectroscopy). We attribute the low binding energy Si2*p* core line at 103.5 eV in the thick film (or 101.8 eV in the thin film) to a multicomponent peak consisting of "bulk" Si, and one or more of Si–C, Si–H, and Si^{1+}—in which one Si–Si bond has been replaced by a Si–O bond[28] (the reported value for the Si2*p* binding energy in SiC is 0.9 eV above the main line[29]). As mentioned, recent IR studies of silicon nanocrystallites reveal the formation of SiC bonds,[8] so the presence of a component related to Si–C bonding in the low binding-energy peak cannot be ruled out. In addition, transmission IR experiments on thermal hydrosilylation of porous silicon (the method used to passivate the Si–NCs in our work) shows that the maximum coverage of alkyl chains on porous silicon is 0.3–0.5 ML (monolayer).[30] This suggests that a substantial fraction of the surface atoms of the Si–NCs are bound to hydrogen, but the small difference in binding energy between elemental Si and surface Si bound to hydrogen prevents us from resolving the respective Si2*p* lines.[31,32] The multicomponent nature of the low binding-energy peak consequently prevents a clear observation of the spin-orbit splitting which would be expected from the Si2*p* core level. The evolution of the second peak in the spectra from the slow surfaces is somewhat similar to that observed during the thermal oxidation of Si(001) by Yoshigoe *et al.*:[33] a peak at higher binding energy than the elemental silicon line is observed to increase in intensity, and its centroid increase in binding energy, as a function of oxidation time. Similarly, Lehner *et al.* showed that upon exposure of H-passivated Si(111) to ambient atmosphere a broad peak appeared at about 2.7 eV above the main Si line, evolving in intensity and binding energy as a function of time.[34] It is therefore reasonable to assign the high binding-energy peak which appears in the slow samples to the photon-induced formation of a number of (sub)oxide species (SiO_x, where $x \leqslant 2$). The evolution of the intensity and position of this peak therefore indicates that, as irradiation progresses, the coverage of surface oxide and the average oxidation state of the silicon atoms at the surface of the nanocrystals increase, which agrees well with the sequential appearance of successively higher Si oxidation states during thermally driven oxidation.[33]

Our attribution of the higher binding-energy peak in spectra from the slow samples to photoinduced oxidation is supported by results of recent VUV surface photochemical studies of water adsorbed on graphite[35] and CO_2 ice.[36] It was shown that $H^+(D^+)$ and $H_3O^+(D_3O^+)$ ion fragments can readily desorb into vacuum, leaving OH species (possibly in an excited state) trapped at the surface and thus available for silicon oxidation. Desorption of hydrogen from Si surfaces can also be induced under VUV photoirradiation[37,38] and the resultant dangling bonds would be able to act as reaction sites. Photoemission studies of the adsorption of water on Si(111)-7×7 and Si(100)-2×1 surfaces have shown that in addition to dissociative adsorption leading to –H and –OH bound to the Si surface, oxidation also exists as an alternative reaction channel.[39] Indeed, silicon oxidation states from +1 through +4 are observed for water adsorption at 90 K, indicating that the activation barrier for oxidation is relatively low.[39] In consequence, photoirradiation of the Si-NCs in the presence of suitable adsorbates (arising from residual atmospheric contamination) can be seen to be a route by which oxidation of the nanocrystals might occur. The absence of the second, oxide, peak in fast samples [compare Figs. 3(a) and 4(a)] can be explained by the time required for diffusion of water (and/or oxygen, carbon dioxide, etc.) into the samples from the ambient atmosphere. It must be borne in mind that the as-prepared samples contain significant quantities of the original solvent which must diffuse out or undergo exchange with water during atmospheric exposure in order for there to be a sufficient concentration of the latter within the film to enable photoinduced oxidation to occur.

Figure 6 shows the room-temperature photoluminescence spectrum of the fast sample excited by synchrotron radiation at $h\nu = 106.5$ eV. This particular photon energy has been used because near-edge x-ray-absorption fine-structure (NEXAFS) measurements exhibit the most pronounced peak at this energy (not shown here). The luminescence spectrum exhibits two distinct peaks, blue at 390 ± 20 nm and green at 480 ± 20 nm, and a broad continuum extending into the orange region. The straight line shown in Fig. 6 is a base line, corresponding to zero intensity. The orange light, also observed in our previous work on laser-induced PL in the

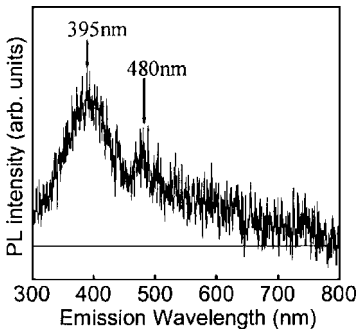

FIG. 6. Room-temperature photoluminescence spectrum (PL) from a "fast" sample excited by synchrotron radiation at $h\nu$=106.5 eV.

nanocrystallites,[8] originates from quantum confinement and Si–Si bonding. We attribute the blue/green emission to transitions which are not strongly dependent on the size of the nanocrystallites, such as excitation of Si–O species. In this work data were obtained using excitation with 106.5-eV photons; at this energy it is known that absorption is related to Si–O bonding.[40] The dominance of blue luminescence in the spectra shown in Fig. 6 thus provides support to our assignment of the source of the blue/green emission. The emission of green light may also be associated with the presence of nitrogen, originating from exposure to ambient atmosphere, trapped within the carbon chains. A similar conclusion has been recently drawn in an XEOL study of oxide-capped Si nanowires.[41]

Figure 7(a) shows a series of narrow region (blue peak) room-temperature PL spectra taken during exposure to synchrotron radiation at $h\nu$=106.5 eV, while Fig. 7(b) plots the resulting decay of the blue peak PL intensity (390-nm emission wavelength) with photoirradiation. The elapsed time between the panels in Fig. 7(a) is about 6 min. The intensity (I_{PL}) decay curve may be fitted by an exponential function $I_{PL}=0.72\exp(-x/1900)$, where $x=\text{flux}\times\text{time(nA s)}$. This behavior indicates that the decay of PL intensity might be related to the decay of intensity of the low binding-energy peak in the Si2p photoemission spectra since both vary exponentially. The differing time constants between the blue PL decay and that of the decay in intensity of the Si2p photoemission peak mean that we are unable to categorically relate both observed decays in intensity to the same process. However, we note that the differences in time constant can, at least in part, be associated with the conditions under which the spectra were obtained. Measurement of the PL process is much less efficient than detection of photoelectrons in terms of counts per incident photon, typically by ~100–1000 times. Hence, for PL measurements the photon fluxes we employed were substantially larger than those used for photoemission spectroscopy. Drain currents on the gold foil at the entrance to the chamber started at 3.01 nA for PL measurements compared with 0.011 nA for photoemission studies. It is known that the total number of emitted electrons (direct photoelectrons and secondaries) due to a single incident photon does not depend linearly upon flux, particularly in the presence of charging, thus the number of trapped electrons within the film will be different in the two cases (PL vs PES). In addition, charging will be distributed over both the

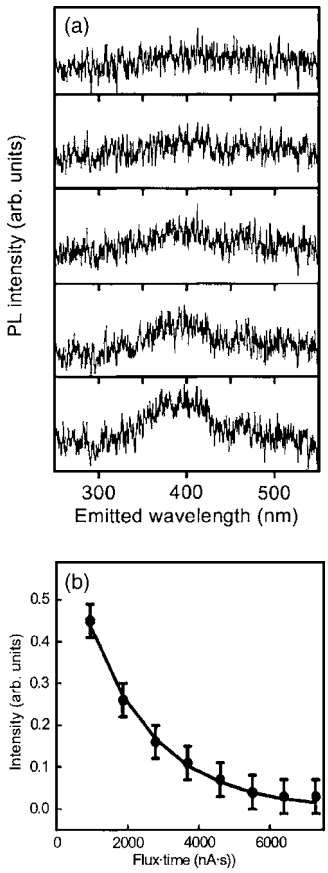

FIG. 7. (a) Room-temperature PL spectra showing the effects of exposure to synchrotron radiation at $h\nu$=106.5 eV. The elapsed time between the panels is the time required to obtain one scan, which is approximately 6 min. (b) Plot of the decay in PL intensity of the blue peak at 390 nm, measured at room temperature as a function of exposure to synchrotron radiation ("fast" sample). The line is an exponential decay fitted to the data.

nanocrystallites and passivating layer (not necessarily in a homogeneous fashion). Charge-induced quenching of the XEOL signal is likely to arise from ionization of the nanocrystallites, as described below. However, charge is also likely to be trapped in the alkyl passivation layer. Charge trapped in the passivating layer is unlikely to participate in the bleaching process (unless located close to the Si–C bond which anchors the alkyl chains to the surface), but such charge will contribute to the local energy barrier experienced by a photoelectron. If we accept that the reduction in intensity in both the PL and Si2p spectra arise from the same source, this suggests that the decay of PL intensity is related to charge trapping phenomena rather than being brought about by the oxidation reaction. The fact that we did not observe any oxidation on the fast sample is a sufficient proof of this, but in addition, the oxidation reaction exhibits a nonexponential growth: see Fig. 4(b), "peak B," for the slow sample.

One of the possible mechanisms by which charging can quench luminescence in alkyl-passivated Si nanocrystallites is described by the "blinking behavior" model advanced by Mason *et al.*,[42] to interpret the luminescence of individual porous Si chromophores. A similar model was also previously used to model the PL of CdSe nanocrystallite quantum dots.[43,44] In this scheme ionization of the semiconductor nanocrystallite liberates a free carrier (a hole produced by

electron emission). Nonradiative decay of further excitations is then possible through energy transfer to this free carrier, quenching luminescence until the nanocrystallite is neutralized. In laser-excited PL measurements ionization occurs through the nonradiative transfer of energy from one exciton to a second trapped near the surface of the quantum dot in an Auger-type process. In XEOL measurements direct photoemission of electrons can occur, creating a more efficient route for the ionization of the nanocrystallites, and consequently bleaching.

CONCLUSIONS

To summarize, alkylated silicon nanocrystallites have been prepared by a combined electrochemical and thermal hydrosilylation process. We imaged these covalently anchored on Si(111) to confirm their size. Si–NCs were deposited from solution as thicker films in order to enable synchrotron-radiation excited photoemission (SRPES) and x-ray excited optical luminescence (XEOL) measurements. During the course of illumination with 145-eV photons we have monitored the evolution of the Si2*p* core level of the Si–NCs, and observed in real time the growth of an extra Si2*p* component. This extra peak is attributed to *in situ* oxidation of the Si nanocrystals brought about by a photoinduced reaction with water (and possibly other contaminants from ambient atmosphere, such as CO_2) which have diffused into nanocrystallite films exposed to the ambient environment for a suitably extended period. XEOL measurements reveal that at least two bands are active upon soft-x-ray photon excitation, and studies of blue band PL indicate that the PL intensity decays exponentially with photoirradiation. We argue that this reduction in PL intensity occurs due to charge trapping arising from the poorly conducting granular nature of the passivated Si–NC film prepared by deposition from solution.

ACKNOWLEDGMENTS

Two of the authors (Y.C.) and (S.K.) are grateful to the scholarship panel of The University of Newcastle for awarding a Development Trust Bursary and an International Research Scholarship, respectively. Two authors (L.Š. and B.R.H.) are grateful to EPSRC for financial support. We acknowledge EC ARI programme support for work undertaken at MAX Lab. We also thank G. Miller for valuable technical support at Daresbury.

[1] J. Valenta, R. Juhasz, and J. Linnros, J. Lumin. **98**, 15 (2002).
[2] M. Buchez, M. Moronne, P. Gin, S. Weiss, and A. P. Alivisatos, Science **281**, 2013 (1998).
[3] F. Cunin, T. A. Schmedake, J. R. Link, Y. Y. Li, J. Koh, S. N. Bhatia, and M. J. Sailor, Nat. Mater. **1**, 39 (2002).
[4] L. Paves, L. dal Negro, C. Mazzoleni, G. Franzo, and F. Priolo, Nature (London) **408**, 440 (2000).
[5] L. Brusm, J. Phys. Chem. **98**, 3575 (1994).
[6] Z. Ding, B. M. Quinn, S. K. Haram, L. E. Pell, B. A. Korgel, and A. J. Bard, Science **296**, 1293 (2002).
[7] J. Valenta, R. Juhasz, and J. Linnros, Appl. Phys. Lett. **80**, 1070 (2002).
[8] L. H. Lie, M. Duerdin, E. M. Tuite, A. Houlton, and B. R. Horrocks, J. Electroanal. Chem. **538/539**, 183 (2002).
[9] L. H. Lie *et al.*, Faraday Discuss. **125**, 235 (2004).
[10] B. Huy, P. H. Binh, B. Q. Diep, and P. V. Luong, Physica E (Amsterdam) **17**, 134 (2003).
[11] H. Elhouichet and M. Oueslati, Appl. Surf. Sci. **191**, 11 (2002).
[12] M. A. Butturi, M. C. Carotta, G. Martinelli, L. Passari, G. M. Youssef, A. Chiorino, and G. Ghiotti, Solid State Commun. **101**, 11 (1997).
[13] Y. Kanemitsu, T. Ogawa, K. Shiraishi, and K. Takeda, Phys. Rev. B **48**, 4883 (1993).
[14] T. Giaddui, L. G. Earwaker, K. S. Forcey, A. Loni, and L. T. Canham, J. Phys. D **31**, 1131 (1998).
[15] X. J. Li, D. L. Zhu, Q. W. Chen, and Y. H. Zhang, Appl. Phys. Lett. **74**, 389 (1999).
[16] T. Giaddui, K. S. Forcey, L. G. Earwaker, A. Loni, L. T. Canham, and A. Halimaoui, J. Phys. D **29**, 1580 (1996).
[17] Y. Kanemitsu, H. Uto, Y. Masumoto, T. Matsumoto, T. Futagi, and H. Mimura, Phys. Rev. B **48**, 2827 (1993).
[18] HRTEM studies show that the nanocrystals have a diameter below about 6 nm, although difficulties in preparation of samples on TEM grids and the low atomic number of Si have so far prevented a more accurate diameter determination by this technique [A. Chuvilin, Yu. Butenko, V. Kuznetsov, L. H. Lie, A. Houlton, B. R. Horrocks, and L. Šiller (unpublished)].
[19] A. R. Pike, L. H. Lie, R. A. Eagling, L. C. Ryder, S. N. Patole, B. A. Connolly, B. R. Horrocks, and A. Houlton, Angew. Chem., Int. Ed. **41**, 615 (2002).
[20] C. G. Cleland, B. R. Horrocks, and A. Houlton, J. Chem. Soc., Faraday Trans. **91**, 4001 (1995).
[21] X-ray data booklet, Lawrence Berkeley National Laboratory, Berkeley, 2001.
[22] In addition to the present evidence, the evaporation of Si–NCs from an evaporation source has been directly measured in ultrahigh vacuum. The comparison of C1*s* photoemission spectra from an evaporated Si–NC film with that from a Si–NC film deposited from solution show that there is no observable degradation of carbon chain upon evaporation [Krishnamurthy *et al.* (unpublished)].
[23] It could be argued that photoemission spectra obtained from a poorly conducting system such as the Si–NC film should be vacuum-level referenced. However, vacuum-level referencing, although changing the absolute values of the "binding energies" quoted, does not change the evolution of the spectra nor the conclusions drawn.
[24] Y. Chao, K. Svensson, D. Radosavkic, V. R. Dhanak, L. Šiller, and M. R. C. Hunt, Phys. Rev. B **64**, 235331 (2001).
[25] A. J. Maxwell, P. A. Brühwiler, D. Arvanitis, J. Hasselström, and N. Mårtensson, Chem. Phys. Lett. **260**, 71 (1996).
[26] B. Hamilton, J. Jacobs, D. A. Hill, R. F. Pettifer, D. Teehan, and L. T. Canham, Nature (London) **393**, 443 (1998).
[27] D. Stauffer and A. Aharony, *Introduction to Percolation Theory* (Taylor and Francis, London, 1994).
[28] F. J. Himpsel, F. R. McFeely, A. Taleb-Ibrahimi, J. A. Yarmoff, and G. Hollinger, Phys. Rev. B **38**, 6084 (1988).
[29] Y. Hijikata, H. Yaguchi, M. Yoshikawa, and S. Yoshida, Appl. Surf. Sci. **184**, 161 (2001).
[30] A. B. Sieval, R. Linke, G. Heij, G. Meijer, H. Zuilhof, and E. J. R. Sudhölter, Langmuir **17**, 2172 (2001).
[31] K. Hricovini *et al.*, Phys. Rev. Lett. **70**, 1992 (1993).
[32] C. Grupp and A. Taleb-Ibrahim, Phys. Rev. B **57**, 6258 (1998).
[33] A. Yoshigoe, K. Moritani, and Y. Teraoka, Appl. Surf. Sci. **216**, 388 (2003).
[34] A. Lehner, G. Steinhoff, M. S. Brandt, M. Eickhoff, and M. Stutzmann, J. Appl. Phys. **94**, 2289 (2003).
[35] S. R. Baggott, K. W. Kolasinski, L. M. A. Perdigao, D. Riedel, Q. M. Guo, and R. E. Palmer, J. Chem. Phys. **117**, 6667 (2002).
[36] L. Šiller, M. T. Sieger, and T. M. Orlando, J. Chem. Phys. **118**, 8898 (2003).
[37] L. Hellner, L. Phillipe, G. Dujardin, M.-J. Ramage, M. Rose, P. Cirkel, and P. Dumas, Nucl. Instrum. Methods Phys. Res. B **78**, 342 (1993).
[38] A. Pusel, U. Wettrauer, and P. Hess, Phys. Rev. Lett. **81**, 645 (1998).
[39] C. Poncey, F. Rochet, G. Dufour, H. Roulet, F. Sirotti, and G. Panaccione, Surf. Sci. **338**, 143 (1995).

[40]A. Bianconi, Surf. Sci. **89**, 41 (1979).
[41]T. K. Sham *et al.*, Phys. Rev. B **70**, 045313 (2004).
[42]M. D. Mason, G. M. Credo, K. D. Weston, and S. K. Buratto, Phys. Rev. Lett. **80**, 5405 (1998).
[43]M. Nirmal, B. O. Dabbousi, M. G. Bawendi, J. J. Macklin, J. K. Trautman, T. D. Harris, and L. E. Brus, Nature (London) **383**, 802 (1996).
[44]S. A. Empedocles, D. J. Noris, and M. G. Bawendi, Phys. Rev. Lett. **77**, 3873 (1996).